2-Methyl-1-hexen-3-yne Lewis Base Stabilized β-Diketonate Copper(I) Complexes: X-ray Structures, Theoretical Study, and Low-Temperature Chemical Vapor Deposition of Copper Metal

T.-Y. Chen,[†,‡] J. Vaissermann,[†,§] E. Ruiz,[||] J. P. Sénateur,[⊥] and P. Doppelt*[,†,‡]

Laboratoire de Chimie Inorganique et Matériaux Moléculaires (CNRS 7071), ESPCI, 10 rue Vauquelin, 75231 Paris Cedex 05, France; Université P. et M. Curie, 4 Place Jussieu, 75231 Paris Cedex 05, France; Departament de Química Inorgànica and Centre de Recerca en Química Teórica (CeRQT), Universitat de Barcelona, Diagonal 647, 08028 Barcelona, Spain; Laboratoire de Matériaux et Génie Physique, INPG (CNRS 5628), rue de la Houille Blanche, 38402 Saint-Martin-d'Hères, France

Received November 27, 2000. Revised Manuscript Received February 20, 2001

Four new β-diketonate copper(I) complexes containing the ene−yne 2-methyl-1-hexen-3-yne (MHY), [Cu(hfac)(MHY)] (hfac = hexafluoroacetylacetonate), [Cu(tfac)(MHY)] (tfac = 1,1,1-trifluoroacetylacetonate), [Cu(pfac)(MHY)] (pfac = perfluoroacetylacetonate), and [Cu(acac)(MHY)] (acac = acetylacetonate), have been synthesized and characterized by FT-IR and ^{1}H and ^{13}C NMR and three of them by an X-ray structural and elemental analysis. In these complexes, the triple bond is η^2-coordinated to the copper atom while the double bond stays free. A theoretical study demonstrates that for these complexes a planar coordination around the copper ion is the most stable, with energy differences of 57.7, 44.9, 39.3, and 62.7 kJ/mol for the acac, tfac, hfac, and pfac complexes, respectively, when compared to a tetrahedral structure, which is another possible coordination mode for Cu(I). We also found that the orbital contribution of the fluorine atoms does not seem to be very relevant for the Cu−alkyne bond, but rather weak fluorine−hydrogen bonds detected in the X-ray structures can explain the following experimentally found stability order:

[Cu(acac)(MHY)] < [Cu(tfac)(MHY)] < [Cu(hfac)(MHY)] = [Cu(pfac)(MHY)]

The decomposition of such compounds to give Cu(0), MHY, and [Cu(β-diketonate)$_2$] seems to indicate a similar thermodynamic stability of the products. However, experimentally the complex with the pfac ligand shows a greater stability while the acac complex decomposes easily. The more stable and volatile compounds are obtained when the β-diketonate ligand is hexafluoropentanedionate, which has been used as a precursor in copper CVD experiments. So, [Cu(hfac)(MHY)] (mp = 13.0 °C, bp = 207.2 °C), which displays a partial pressure of 110 mTorr at 21.3 °C, was used with 5% (wt) of pure MHY as a stabilizing agent. Using a direct liquid injection and vaporizer system, pure copper films were deposited in a cold-wall LPCVD system with helium as carrier gas on 4 in. diameter silicon wafers covered with a 200 nm thick CVD TiN film as a barrier. The copper films were deposited at a precursor vaporization temperature of 85 °C and deposition temperature of 140−300 °C. In this temperature range, the growth rate demonstrates the two usual different regimes: the mass-flow-controlled regime above 220 °C with a growth rate as high as 260 nm/min and the surface-limited regime below this temperature. For this last regime, the activation energy is only around 30 kJ/mol, which is a very low value when compared to what was obtained for processes using other Cu(I) β-diketonates. Shiny, adhesive copper films with a thickness of 500−1000 nm had resistivities of 2.3−4.5 μΩ cm, depending on the substrate temperature. ESCA analysis of the Cu layers revealed that the Cu films were very pure but contained 2.7 atom % of oxygen impurities due to leaks or residual H_2O in the CVD system which were still present after 10 min of Ar sputtering.

Introduction

Chemical vapor deposition (CVD) processes[1] are increasingly important for ULSI (ultra-large-scale integration) metallization and interconnection. The deposition of pure, conformal metal films is required for multilevel devices with ≤0.13 μm features. As previously reported, the electrical resistivity of the interconnects may limit device performance.[2] Low-resistivity metals and low-dielectric-constant materials reduce the RC time constant and lead to improved device performance.[3] Thus, CVD processes for the deposition of low-resistivity metals (i.e., gold, copper, and silver) require the identification and development of low-cost, volatile precursors.

[†] Laboratoire de Chimie Inorganique et Matériaux Moléculaires (CNRS 7071).
[‡] ESPCI.
[§] Université P. et M. Curie.
[||] Universitat de Barcelona.
[⊥] INPG (CNRS 5628).

10.1021/cm0012318 CCC: $20.00
Published on Web 09/20/2001

Earlier research[1,4,5] clearly demonstrated the potential of Lewis base stabilized copper(I) β-diketonate complexes as copper CVD precursors. The reactive copper(I) β-diketonate moiety may be ligated with phosphines[6] or unsaturated organics, such as alkenes,[7] dienes,[8] and alkynes,[9] to obtain an assortment of precursors with different physical−chemical properties. The deposition of pure copper films from the Cu(I) precursors results from a thermally induced disproportionation reaction, shown in eq 1:

$$2Cu^{I}(\beta\text{-diketonate})L \rightarrow Cu^{0} + Cu^{II}(\beta\text{-diketonate})_2 + 2L \quad (1)$$

Since the Lewis base is weakly bound to the Cu center in the complex, the thermal decomposition of these complexes occurs at low temperatures (150−250 °C) and results in the formation of near-bulk copper films. Film resistivities between 1.8 and 2.5 $\mu\Omega$ cm, as opposed to 1.67 $\mu\Omega$ cm for bulk copper, have been reported.[10]

In general, CVD copper processes have utilized vinyltrimethylsilane [Cu(hfac)(VTMS)] (Cupra-select),[7a] which is commercially available, but is a thermally labile material. Other compounds of the same family have demonstrated valuable results.[1,4,5]

In this family of compounds, the physical properties of the precursor are easily varied by chemical substitution and structural modifications. Changing the Lewis base in the copper(I) complex can directly alter the physical state (liquid or solid), the partial pressure, the decomposition temperature, and the long-term stability of the copper precursor. During CVD experiments using [Cu(hfac)(η^2-alkyne) precursors, a less volatile compound was formed in the bubbler along with copper metal.[9c] This unstable compound was thought to be a dinuclear complex in which the alkyne bridges two copper(I) centers in a "butterfly" geometry. To prove this hypothesis, using bis(trimethylsilyl)acetylene (BTMSA), an alkyne ligand bearing strong donating groups on the alkyne bond (C≡C), we successfully isolated a dinuclear copper(I) β-diketonate by direct synthesis. An attractive way to avoid "butterfly-like" labile dimer formation, while the precursor potential is kept, is to deactivate the C≡C bond with electron-withdrawing groups such as a conjugated double bond, $-OCH_3$, or $-CF_3$ groups. It has been shown that the best results are obtained when the triple bond is conjugated to a double bond.[5]

Hence, [Cu(I)(β-diketonate)(ene−yne)] complexes have been mentioned as powerful precursors for Cu CVD, in particular [Cu(hfac)(MHY)] (MHY = 2-methyl-1-hexen-3-yne).[11−16] In this paper, we report X-ray structural studies of the latter compound and of sister β-diketonate molecules containing MHY, theoretical calculations, and finally a complete CVD study using [Cu(hfac)(MHY)].

Experimental Section

Synthesis and Characterization of Copper (I) Complexes. All the starting materials were commercially available. Infrared spectra were obtained using a Perkin-Elmer 1600 Series FT-IR spectrophotometer. The spectra were obtained neat between two NaCl plates or in Nujol. ^{1}H and ^{13}C{^{1}H} NMR spectra were recorded in $CDCl_3$ (99.8% D from CEA) with a Bruker Instrument AC 300 spectrometer at frequencies of 300 and 75 MHz, respectively, and chemical shifts are reported in ppm (δ) downfield of TMS with residual protonated $CHCl_3$ as internal standart (δ 7.26 ppm for ^{1}H, δ 77.0 ppm for ^{13}C). Multiplicities are indicated by s (singulet), d (doublet), t (triplet), or q (quartet). UV−vis spectra were obtained using a UVIKON 860 (Kontron Instrument). The melting and boiling points were determined either by DSC (differential scanning calorimetry, DSC7 from Perkin-Elmer) in the case of [Cu(hfac)(MHY)] or by usual methods for the other compounds. Elemental analyses were performed by the Service Central d'Analyze du CNRS (Vernaison, France).

The system used for vapor pressure measurements of precursor compounds is described in another paper.[17] It is a static system very well suited to air- and temperature-sensible compounds. All the components of the ultrahigh vacuum (UHV) material were made in 304L stainless steel and equipped with Conflat (CF) flanges. The sample was loaded in a glass container welded to a stainless steel flange. After pumping with a turbomolecular pumping station, the vapor pressures were measured by means of a capacitance gauge (Edwards Barocell 622) working in the pressure range of 10^{-1}−10^3 Pa (0.001−10 Torr), with a reading accuracy of 0.15%.

Synthesis of [Cu(hfac)(MHY)]. The following reaction was carried out under a steady flow of nitrogen; although the complex is slightly O_2 sensitive, it is not necessary to purge the solution prior to initiation of the synthetic reaction. A three-neck round-bottom flask was loaded with 3 g (21 mmol) of Cu_2O (Aldrich) and 25 mL of spectroscopic grade pentane. 1,1,1,5,5,5-Hexafluoroacetylacetone (3.2 mL, 23 mmol, ABCR) was added dropwise to the magnetically stirred solution that contained 2.9 mL (23.4 mmol) of 2-methyl-1-hexen-3-yne (MHY, ABCR). The reaction was stirred throughout the addition and for 30 min after the addition was completed. The brick-red cuprous oxide was suspended in the clear solution that became yellow-green as the reaction proceeded. Excess Cu_2O was filtered off and the pentane solution purified by flash chromatography under nitrogen with a 1.3 in. (diameter) by 5 in. (height) alumina column (6 g). After chromatography and

(1) Kodas, T. T.; Hampden-Smith, M. J., Eds. *The Chemistry of Metal CVD;* VCH Publishers: New York, 1994.
(2) Pai, P. L.; Ting, C. H. *IEEE Electron Dev. Lett.* **1989**, *10*, 423.
(3) Small, M. B.; Pearson, D. J. *IBM J. Res. Dev.* **1990**, *34***,** 858.
(4) Doppelt, P.; Baum, T. H. *MRS Bull.* **1994**, *XIX* (8), 41.
(5) Doppelt, P. *Coordination Chem. Rev.* **1998**, *180* (1−3), 1783.
(6) (a) Jain, A.; Chi, K.-M.; Kodas, T. T.; Hampden-Smith, M. J.; Farr, J. D.; Pafett, M. F. *Chem. Mater.* **1991**, *3*, 995. (b) Shin, H.-K.; Hampdem-Smith, M. J.; Kodas, T. T.; Duesler, E. N. *Polyhedron* **1991**, *10*, 645.
(7) (a) Norman, J. A. T.; Muratore, B. A.; Dyer, P. N.; Roberts, D. A.; Hochberg, A. K. *J. Phys. IV (Paris)* **1991**, C2−271. (b) Jun, C.-H.; Kim, Y. T.; Baek, J.-T.; Yoon, H. J.; Kim, D.-R. *J. Vac. Sci. Technol.* **1996**, A 14 (6), 3214. (c) Park, M.-Y.; Son, J.-H.; Rhee S.-W. *Electrochem. Solid-State Lett.* **1998**, *1*, 32. (d) Son, J.-H.; Park, M.-Y.; Rhee S.-W. *Thin Solid films* **1998**, *335*, 229. (e) Senzaki, Y. *J. Electrochem. Soc.* **1998**, *145*, 362. (f) Rhee, S.-W.; Kang, S.-W.; Han, S.-H. *Electrochem. Solid-State Lett.* **2000**, *3*, 135.
(8) (a) Reynolds, S. K.; Smart, C. J.; Baran, E. F.; Baum, T. H.; Larson C. E.; Brock, P. J. *Appl. Phys. Lett.* **1992**, *59*, 2332. (b) Doppelt, P.; Baum, T. H.; Ricard, L. *Inorg. Chem.* **1996**, *35*, 1286.
(9) (a) Baum T. H.; Larson, C. E., *Chem. Mater.* **1992**, *4*, 365. (b) Baum, T. H.; Larson, C. E. *J. Electrochem. Soc.* **1993**, *140*, 154. (c) Doppelt, P.; Baum, T. H. *J. Organomet. Chem.* **1996**, *517*, 53.
(10) Pehrsen, G. A.; Parmehr, J. E.; Apblett, C. A.; Gonzales, M. F.; Smith, P. M.; Omslead, T. R.; Norman, J. A. T. *J. Electrochem. Soc.* **1995**, *142*, 939.
(11) Doppelt, P. French Patent 97 03 029, US Patent 6,130,345.
(12) Combellas, C.; Doppelt, P.; Kanoufi, F.; Chen, T.-Y.; Thiebault, A. *Chem. Vap. Deposition* **1999**, *5*, 185.
(13) Doppelt, P.; Chen, T.-Y.; Madar, R.; Torres, J. *AMC 98, MRS Proceedings* **1999**, 117.
(14) Vidal, S.; Maury, F.; Gleizes, A.; Chen, T.-Y.; Doppelt, P. *J. Physique* C **1999**, *9*, Pr8−791.
(15) Nguyen, T.; Charneski, L.; J. Hsu, S. T.; Bhandari, G. *AMC 98, MRS Proceedings* **1999**, 147.
(16) Zhang, J.; Denning, D.; Braeckelmann, G.; Hamilton, G.; Lee, J. J.; Venkatraman, R.; Fiordalice, B.; Weitzman, E. *Mater. Res. Soc. Symp. Proc.* **1999**, *564*, 243.
(17) Cicoira, F.; Ohta, T.; Doppelt, P.; Beitone, L.; Hoffmann, P. *Chem. Vap. Deposition*, **2001** in press.

distillation of the solvent, the yellow liquid, [Cu(hfac)(MHY)], was obtained typically with a 90% yield (based on hfac). (DSC: sample weight = 5.8 mg, scanning rate = 20.0 °C/min, mp = 13.0 °C (ΔH = 39.5 J/g), bp = 207 °C (ΔH = 27.0 J/g). IR (neat): 2983 (w), 2945 (w), 2883 (w) 2017 (w, C≡C), 1641 (s), 1602 (m), 1556 (m), 1528 (m), 1476 (s), 1348 (w), 1262 (s), 1202 (s), 1145 (s), 1103 (w), 917 (w), 799 (m), 745 (w), 674 (m), 589 (m) cm^{-1}. ^1H NMR ($CDCl_3$, 298 K) δ (ppm): 1.35 (t, 7.4 Hz, CH_3), 2.08 (s, CH_3), 2.72 (q, 7.4 Hz, CH_2), 5.43 (d, 72.1 Hz, $=CH_2$), 6.17 (s, C−H, hfac). $^{13}C\{^1H\}$ NMR ($CDCl_3$, 298 K) δ (ppm): 13.7 (*C*H_3), 16.3 (*C*H_3), 23.8 (*C*H_2), 87.8 (*C*≡C), 89.9 (*C*−H), 95.9 (C≡*C*), 117.82 (q, J_{CF} = 283.5 Hz, *C*F_3), 120.3 (C=*CH*$_2$), 125.5 (−*C*=C), 178.4 (q, J_{CF} = 34.4 Hz, *C*=O). ^{19}F NMR ($CFCl_3$ as a standard) δ (ppm): −76.9. Anal. Calcd for $C_{12}H_{11}F_6O_2Cu$: C, 39.51, H, 3.04, Cu, 17.4. Found: C, 40.0 H, 3.10, Cu, 17.0. Yellow crystals of [Cu(hfac)(MHY)] were grown at 5 °C by sublimation (5×10^{-2} mbar) for X-ray analysis.

Synthesis of [Cu(tfac)(MHY)]. The same procedure as for [Cu(hfac)(MHY)] was used except 2.8 mL of 1,1,1-trifluoroacetylacetone (ABCR) was used instead of 1,1,1,5,5,5-hexafluoroacetylacetone. The white solid was prepared in 72% yield (based on tfac). Mp = 57 °C. IR (Nujol): 2020 (w, C≡C), 1618 (s), 1560 (w), 1542 (w), 1523 (m), 1297 (s), 1224 (s), 1191 (s), 1141 (s), 916 (w), 861 (m), 779 (w), 732 (w), 670 (w) cm^{-1}. ^1H NMR ($CDCl_3$, 298 K) δ (ppm): 1.30 (t, 7.4 Hz, CH_3), 2.04 (s, CH_3), 2.13 (s, CH_3 on tfac), 2.67 (q, 7.4 Hz $-CH_2-$), 5.23 (s, =CH*H*), 5.55 (s, =CH*H*), 5.76 (s, C−H, hfac). $^{13}C\{^1H\}$ NMR ($CDCl_3$, 298 K) δ (ppm): 13.9 (*C*H_3), 16.2 (*C*H_2), 23.9 (CH_3), 29.2 (CH_3 on tfac), 88.1 (*C*≡C), 95.0 (*C*−H), 96.5 (C≡*C*), 118.9 (q, J_{CF} = 283 Hz, *C*F_3), 119.2 (=CH_2), 125.4 (−C=), 170.9 (q, J_{CF} = 32 Hz, *C*=O), 198.4 (s, *C*=O). Anal. Calcd for $C_{12}H_{14}F_3O_2Cu$: C, 46.38, H, 4.54, F, 18.34. Found: C, 46.30, H, 4.28, F, 18.52. Translucent crystals of [Cu(tfac)(MHY)] were grown at 5 °C by sublimation (5×10^{-2} mbar) for X-ray analysis.

Synthesis of [Cu(pfac)(MHY)]. A bright yellow liquid, [Cu(pfac)(MHY)], was prepared in 87% yield (based on pfac) with a procedure analogous to that for the synthesis of [Cu(hfac)(MHY)] except 5.2 g of 1,1,1,3,5,5,5-heptafluoropentane-2,4-dione (ABCR) was used instead of 1,1,1,5,5,5-hexafluoroacetylacetone. Mp = 31 °C. IR (neat): 3290 (w), 3103 (w), 2985 (f), 2946 (w), 2886 (w), 2020 (w, C≡C), 1648 (s), 1624 (m), 1560 (w), 1508 (m), 1475 (s), 1458 (s), 1348 (w), 1376 (w), 1352 (w), 1271 (s), 1194 (s), 1153 (s), 1086 (w), 1059 (w), 1010 (w), 917 (m), 812 (w), 761 (m), 677 (m), 599 (s) cm^{-1}. ^1H NMR ($CDCl_3$, 298 K) δ (ppm): 1.33 (t, 7.4 Hz, CH_3), 2.06 (s, $-CH_3$), 2.71 (q, 7.5 Hz, CH_2), 5.34 (s, =CH*H*), 5.55 (s, =CH*H*). $^{13}C\{^1H\}$ NMR ($CDCl_3$, 298 K), δ (ppm): 13.8 (*C*H_3), 16.3 (*C*H_2), 23.8 (*C*H_3), 87.4 (*C*≡C), 95.4 (C≡*C*), 117.9 (q, J_{CF} = 285 Hz, *C*F_3), 121.5 (=*C*H_2), 125.4 (=*C*−), 141.8 (d, J_{CF} = 230 Hz, =*C*−F), 168.3 (q, J_{CF} = 32 Hz, *C*=O). Anal. Calcd for $C_{12}H_{10}F_7O_2Cu$: C, 37.65, H, 2.63, F, 34.75. Found: C, 37.16, H, 2.55, F, 34.75. Yellow crystals of [Cu(pfac)(MHY)] were grown at 5 °C by sublimation (5×10^{-2} mbar) for X-ray analysis.

Synthesis of [Cu(acac)(MHY)]. A Schlenk flask was loaded with 3 g (30 mmol) of CuCl (Aldrich) and 3.5 mL (28 mmol) of MHY and 30 mL of dried THF was stirred in. The mixture was stirred for 20 min. Na(acetylacetonate) (3.2 g, 26 mmol; Aldrich) was added to the solution and continuously stirred for an additional 1 h. Removal of volatile species in a vacuum (oil pump, 1 mBar) gave a white-gray residue. The product was extracted from the residue with pentane; the solvent was removed in a vacuum (oil pump, 1 mbar) to give the white solid [Cu(acac)(MHY)] with a 63% yield (based on acac). Mp = 75 °C. IR (Nujol): 1994 (C≡C, w), 1588 (s), 1560 (m), 1542 (m), 1522 (s), 1400 (s), 1264 (m), 1195 (w), 1079 (w), 1018 (m), 915 (m), 890 (w), 770 (m), 670 (w), 654 (w), 579 (m) cm^{-1}. ^1H NMR ($CDCl_3$, 298 K) δ (ppm): 1.24 (t, 7,0.4 Hz, $-CH_3$), 1.91 (s, $-CH_3$ on acac), 1.97 (s, $-CH_3$), 2.57 (q, 7.4 Hz, $-CH_2-$), 5.10 (s, =CH*H*), 5.31 (s, =CH*H*), 5.43 (s, −CH on acac). $^{13}C\{^1H\}$ NMR ($CDCl_3$, 298 K) δ (ppm): 13.9 (*C*H_3), 16.1 (*C*H_2), 23.8 (*C*H_3), 27.8 (*C*H_3 on acac), 88.5 (*C*≡), 96.9 (≡*C*), 99.6 (*C*H on acac), 117.1 (=*C*H_2), 124.71 (*C*=), 190.3 (*C*=O). Due to the instability of the complex, no satisfactory elemental analysis was obtained.

Table 1. Crystal and Intensity Collection Data for [Cu(hfac)(MHY)], [Cu(tfac)(MHY)], and [Cu(pfac)(MHY)]

	[Cu(hfac)(MHY)]	[Cu(tfac)(MHY)]	[Cu(pfac)(MHY)]
formula	$C_{12}H_{11}F_6O_2Cu$	$C_{12}H_{14}F_3O_2Cu$	$C_{12}H_{10}F_7O_2Cu$
formula weight, amu	364.75	310.78	382.74
crystal habit, color	block, yellow	block, translucent	block, yellow
crystal system	monoclinic	triclinic	monoclinic
space group	*P*21/*n*	P**1**	*P*21/*n*
a, Å	11.498(6)	6.918(4)	7.321(5)
b, Å	16.858(12)	10.654(7)	20.313(11)
c, Å	15.235(3)	10.884(3)	9.868(6)
α, deg		63.28(4)	
β, deg	104.90(10)	71.44(4)	93.26(5)
γ, deg		71.07(5)	
V, Å^3	2854(6)	663.5(7)	1465(2)
Z	8	2	4
D_{calcd}, g cm^3	1.70	1.56	1.74
temperature, K	230	238	223
λ, Å	0.71069	0.71069	0.71069
no. data measured	5491	2878	2537
no. data with $I > 3.00\,\sigma(I)$	1684	1358	1555
R[a]	0.0697	0.0521	0.0499
R_w[b]	0.0801	0.0632	0.0602

[a] $R = \sum||F_o| - |F_c||/\sum|F_o|$. [b] $R_w = [\sum w||F_o| - |F_c||^2/\sum w|F_o|^2]^{1/2}$.

X-ray Crystallographic Analysis for [Cu(hfac)(MHY)], [Cu(tfac)(MHY)], and [Cu(pfac)(MHY)]. The crystals were picked directly from the Schlenk flask under cold nitrogen flow and glued to the top of a glass needle with Araldite. Data collection was performed on an Enraf-Nonius MACH-3 diffractometer with the crystal maintained in a cold nitrogen flow. Crystals, data collection, and refinement parameters are given in Table 1. Accurate cell dimensions and orientation matrixes were obtained by least-squares refinements of 25 accurately centered reflections. No significant variations were observed in the intensities of two separate reflections during data collection. The data were corrected for Lorentz and polarization effects. Computations were performed using the PC version of CRYSTALS[18] Scattering factors and corrections for anomalous absorption were taken from ref 19. The structures were solved by direct methods (SHELXS[20,21]). The final refinements were carried out by full-matrix least-squares using anisotropic displacement parameters for all non-hydrogen atoms. Hydrogen atoms were introduced at calculated positions and only one overall isotropic displacement parameter was refined.

Computational Details. A theoretical study devoted to this family of organometallic compounds was carried out using methods based on density functional theory. These methods provide an excellent compromise between accuracy and computer time, being particularly suitable for transition metal complexes.[22] All the results presented were obtained using the Gaussian98 program.[23] The hybrid B3LYP method[24] was used in all calculations as implemented in Gaussian code mixing the exact Hartree−Fock-type exchange with Becke's expression for the exchange functional[25] and the Lee−Yang−Parr correlation functional.[26] A basis set of double-*ς* quality (including two additional p functions for the Cu atoms) proposed by Schaefer et al.[27] was employed throughout, together with the default grid to compute the exchange-correlation potentials and energies using the numerical integration weighting scheme

(18) Watkin, D. J.; Prout, C. K.; Carruthers, J. R.; Betteridge, P. W. *Crystals*; Chemical Crystallography Laboratory, University of Oxford: Oxford, U.K. 1996; Issue 10.

(19) Cromer D. T. *International Tables for X-ray Crystallography*; Kynoch Press: Birmingham, U.K. 1974; Vol. IV.

(20) Sheldrick, G. H. *SHELXS-86. Program for Crystal Structure Solution*; University of Gottingen: Gottingen, Germany, 1986.

(21) Watkin, D. J.; Prout, C. K.; Pearce, L. J. *Cameron*; Crystallography Laboratory University of Oxford: Oxford, U.K., 1996.

(22) Koch, W.; Holthausen, M. C. *A Chemist's Guide to Density Functional Theory*; Wiley-VCH Verlag: Weinheim, 2000.

proposed by Scuseria and Stratman.[28] We performed calculations with the Spartan[29] and Jaguar[30] codes to confirm the results of the stationary points search. The basis set superimposition error in the calculated interaction energies was corrected using the usual counterpoise method. The vertical excitation energies were calculated using a method based on the time-dependent density functional theory (TD-DFT)[31,32] as implemented in the Gaussian code. Recently, various authors have shown the ability of such a procedure to estimate electronic transition energies for compounds including transition metal atoms.[33,34]

Cu CVD Experiments. Chemical vapor deposition experiments were performed in a prototype LPCVD single-wafer warm-walled bell jar reactor (125 mm) equipped with a "JIPELEC INJECT SYSTEM". The CVD chamber was made of glass and had a diameter of about 180 mm and a height of about 220 mm. The chamber was exhausted by an oil primary pump connected to a cold trap. The mixture of [Cu(hfac)(MHY)] with 5% (wt) of pure MHY was introduced directly into the reactor by injection. The principle of the method involves the computer-controlled injection of micro quantities of liquid (2 μL) precursor inside an evaporator. The droplets injected are immediately vaporized and the vapor transported by a carrier gas to the reaction region, where the substrate is positioned. The liquid was kept at room temperature in a glass reservoir connected to the back of the injector and pressurized under 1 bar of helium. The droplets were injected into an evaporator (held at 85 °C) at a frequency of one or two injection(s)/s with an injector opening time of 0.5 ms corresponding to a precursor flow of 0.23 and 0.46 g/min, respectively. Typical deposition times were on the order of 10 min, corresponding to 600/1200 injections. Helium was used as carrier gas (90 sccm). The reactor walls were heated to 100 °C. The overall pressure inside the reactor was 2 Torr. The substrate was heated by resistance. Its temperature was measured with a calibrated thermocouple placed in the rear of the susceptor. Films were deposited on 4 in. silicon wafers that had preliminary received a 200 nm TiN coat deposited by CVD (thermally with TDMAT and treated with H_2 plasma). As a vacuum break is necessary in our setup, the TiN surface was cleaned with a HF solution to remove any residual oxide.[35] The experiments were performed over a substrate temperature range of 140−300 °C. The films were cooled in He before exposure to air and analyzed by various techniques. No other additives were used during the deposition experiments; in particular, no water was added.

The XPS spectra (Al Kα; primary radiation 1486 eV) were recorded with a VG Scientific Ltd Escalab 220i. The spectrometer was operated in the constant band-pass energy mode (20 eV). Most of the measurements were made at an angle of 90° to the surface. The spectra were corrected for sample charging, the C 1s peak of adventitious carbon (285.0 eV) being used as the reference. The atomic concentrations of fluorine and oxygen relative to carbon were calculated by comparing the intensities of the specific peaks and taking into account their relative atomic sensitivity factors. A JEOL JSM-5200 scanning electron microscope (SEM) operating at an accelerating voltage of 5 kV was used to examine film morphology. The film thickness was measured with an Alpha-Step Tencor Profiler profilometer. The thickness used for the film growth rate was the average of four measurements performed at different places on a scratch drawn by hand with a diamond tip. The precision of the measurements was ±10%.

The sheet electrical resistance of the films was measured at room temperature with a standard four-point technique homemade instrument. Each measurement was performed four times.

Results and Discussion

Synthesis and Charaterization of [Cu(hfac)(MHY)], [Cu(pfac)(MHY)], [Cu(tfac)(MHY)], and [Cu(acac)(MHY)]. Four new compounds were synthesized and characterized by NMR, IR, UV−vis, and elementary analysis (except [Cu(acac)(MHY)]). All of them were characterized by an X-ray structural and elementary analysis except [Cu(acac)(MHY)], for which no satisfactory single crystals were obtained. Synthesis of the compounds was inspired by previously reported methods, either by reaction of Cu_2O on the free acid β-diketone in the presence of MHY[4,8b] or by reaction of CuCl on the sodium β-diketonate when the corresponding β-diketone was not acidic enough to react with Cu_2O (as was the case with Hacac).[1,4]

Their melting points varied from 13 °C for [Cu(hfac)(MHY)] to 75 °C for [Cu(acac)(MHY)]. In the case of [Cu(hfac)(MHY)] the DSC trace[11] gave the mp as 13.0 °C (ΔH = 39.5J/g); the onset of decomposition happened at approximately 140 °C, but the compound was stable enough to reach its bp (207.2 °C, ΔH = 27.0 J/g). The vapor pressure of [Cu(hfac)(MHY)] and [Cu(pfac)(MHY)] are respectively 0.11 Torr (14.5 Pa) at 21.3 °C and 0.065 Torr (8.7 Pa) at 22.4 °C. A complete vapor pressure study will be given elsewhere.[33] Obviously, the presence of the seventh fluoride on the complex does not increase its volatility. [Cu(hfac)(MHY)] is less volatile than [Cu(hfac)(VTMS)] (VTMS = vinyltrimethylsilane) or [Cu(hfac)(DMB)][7c,7f] (DMB = 3,3-dimethyl-1-butene), but this is not a real obstacle to obtain high growth rate during copper deposition as described later. All the compounds were slightly air-sensitive and thermally unstable. Experimentally, the order of stability was found to be

$$[\text{Cu(acac)(MHY)}] < [\text{Cu(tfac)(MHY)}] < [\text{Cu(hfac)(MHY)}] = [\text{Cu(pfac)(MHY)}]$$

[Cu(hfac)(MHY)] is one of the more stable compounds of the series. As it is also the most volatile and occurs as a liquid at room temperature, most of the work was performed using this precursor. Its thermal stability was evaluated in more detail by heating a sealed vial

(23) Frisch, M. J.; Trucks, G. W.; Schlegel, H. B.; Scuseria, G. E.; Robb, M. A.; Cheeseman, J. R.; Zakrzewski, V. G.; Montgomery, J. A., Jr.; Stratmann, R. E.; Burant, J. C.; Dapprich, S.; Millam, J. M.; Daniels, A. D.; Kudin, K. N.; Strain, M. C.; Farkas, O.; Tomasi, J.; Barone, V.; Cossi, M.; Cammi, R.; Mennucci, B.; Pomelli, C.; Adamo, C.; Clifford, S.; Ochterski, J.; Petersson, G. A.; Ayala, P. Y.; Cui, Q.; Morokuma, K.; Malick, D. K.; Rabuck, A. D.; Raghavachari, K.; Foresman, J. B.; Cioslowski, J.; Ortiz, J. V.; Stefanov, B. B.; Liu, G.; Liashenko, A.; Piskorz, P.; Komaromi, I.; Gomperts, R.; Martin, R. L.; Fox, D. J.; Keith, T.; Al-Laham, M. A.; Peng, C. Y.; Nanayakkara, A.; Gonzalez, C.; Challacombe, M.; Gill, P. M. W.; Johnson, B. G.; Chen, W.; Wong, M. W.; Andres, J. L.; Head-Gordon, M.; Replogle, E. S.; Pople, J. A. *Gaussian 98*; Gaussian, Inc.: Pittsburgh, PA, 1998.

(24) Becke, A. D. *J. Chem. Phys.* **1993**, *98*, 5648.

(25) Becke, A. D. *Phys. Rev. A* **1988**, *38*, 3098.

(26) Lee, C.; Yang, W.; Parr, R. G. *Phys. Rev. B* **1988**, *37*, 785.

(27) Schaefer, A.; Horn, H.; Ahlrichs, R. *J. Chem. Phys.* **1992**, *97*, 2571.

(28) Stratmann, E.; Scuseria, G. E.; Frisch, M. J. *Chem. Phys. Lett.* **1997**, *257*, 213.

(29) *Spartan*, version 5.0, Wave function Inc.: Irvine, CA, 1997.

(30) *Jaguar*, version 4.0, Schrodinger Inc.: Portland, OR, 1998.

(31) Casida, M. Time Dependent Density Functional Response Theory for Molecules. In *Recent Advances in Density Functional Methods*; Chong, D. P., Ed.; World Scientific: Singapore, 1995.

(32) Jamorski, C.; Casida, M.; Salahub, D. R. *J. Chem. Phys.* **1996**, *104*, 5134.

(33) Rosa, A.; Baerends, E. J.; van Gisbergen, S. J. A.; van Lenthe, E.; Groeneveld, J. A.; Snijders, J. G. *J. Am. Chem. Soc.* **1999**, *121*, 10356.

(34) van Gisbergen, S. J. A.; Groeneveld, J. A.; Rosa, A.; Snijders, J. G.; Baerends, E. J. *J. Phys. Chem. A* **1999**, *103*, 6835

(35) Hanaoka, K.-I.; Ohnishi, H.; Tachibana, K. *Jpn. J. Appl. Phys.* **1995**, *34*, 2430.

Table 2. Experimental Frequencies for the Complexes Studied Indicating the Frequency Shift Corresponding to the Triple Bond of the Alkyne and the Equivalent Calculated Value and Experimentally Determined Chemical Shift and Coordination Chemical Shift ($\Delta\delta_{C\equiv C}$) Obtained from $^{13}C\{^1H\}$ NMR of Free MHY and [Cu(β-diketonate)(MHY)]

[Cu(β-diketonate)(MHY)]	acac	tfac	hfac	pfac	free MHY
$\nu_{C\equiv C}$ (cm^{-1})	1994	2003	2018	2020	2230
$\Delta\nu_{C\equiv C}$ exp	−236	−227	−212	−210	
$\Delta\nu_{C\equiv C}$ calc	−266	−255	−246	−243	
$\delta_{C\equiv C}$ (ppm)	88.5 96.9	88.1 96.5	87.8 95.9	87.4 95.4	81.1 90.6
$\Delta\delta_{C\equiv C}$ (ppm)	7.4 6.3	7 6.7	6.7 5.3	6.3 4.8	

containing the pure compound or a mixture of the pure compound with the corresponding free base (98/2% w) in an oven. For example, pure [Cu(hfac)(MHY)] can withstand 4 h at 65 °C. The mixture with the free base can be kept for 2 days under the same conditions.

In all cases, the 1:1 Cu(β-diketonate)−MHY stoichiometry was checked by ^1H NMR. The ^{13}C NMR spectra demonstrate that the ligand is bound to the metal center via the triple bond while the double bond stays free. The dominant bonding mode in the alkyne−metal complexes may be evaluated by vibrational spectroscopy (IR) and NMR spectral shift as previously reported[9c,37] and can be influenced by the number of fluorine atoms present on the ancillary ligand (n_F). The strength of the (η^2-C≡C)−Cu bond, the most fragile bond of the structure, and hence the stability of the complex is dependent on the (C≡C) bond contribution. In Table 2, we report the ^{13}C NMR spectra of the series β-diketonate−copper−MHY complexes and compare the chemical shifts of the free MHY with the copper coordinated alkyne. Also, IR spectroscopy may be used to evaluate alkyne−metal bonding. Table 2 also compares the 'free' alkyne stretch frequencies ($\nu_{C\equiv C}$) to those in the copper(I) β-diketonato complexes. Alkyne−transition metal bonding usually decreases the bond order of the alkyne (from sp to sp^2) and thereby lowers the frequency of the alkyne stretching vibration ($\Delta\nu$).[9c,37] The magnitude of this change is directly related to the alkyne bond order and nuclearity of the complex. Relatively small frequency changes ($\Delta\nu \cong 200$ cm^{-1}) are observed for the [Cu(β-diketonate)(MHY)] complexes reported herein as for other [Cu(hfac)(alkyne)] complexes. The $\Delta\nu$ are relatively close, but a trend depending on n_F can be observed: the higher the n_F, the closer the IR C≡C vibration of the complex to that of free MHY. The same trend is observed for the $\Delta\delta$ obtained in ^{13}C NMR spectra, where $\Delta\delta$ represents the experimentally measured chemical shift and coordination chemical shift. Surprisingly, the results reveal that the (η^2-C≡C)−Cu bond strength decreases as n_F increases, which is in contradiction with what has been reported so far.[4,5] We will discuss this topic in the paragraph devoted to the theoretical calculation.

Crystal Structures of [Cu(hfac)(MHY)], [Cu(pfac) (MHY)], and [Cu(tfac)(MHY)]. The asymmetric unit of [Cu(hfac)(MHY)] contains two independent molecules, A and B. One of the X-ray crystallographic molecular structures of [Cu(hfac)(MHY)] is displayed in Figure 1. The relevant bond distances and angles are listed in Table 3. The structure of [Cu(hfac)(MHY)] is not very precise, due to the low melting point of the product (13 °C) and to sublimation or decomposition of the crystal during data collection, even at low temperature (−120 °C). A and B structures are slighly different but roughly similar to that of [Cu(hfac)(η^2-butyne)] [9a] and [Cu(hfac)(BTMSA)] (BTMSA = bis(trimethylsilyl)-acetylene).[9c] The copper−alkyne−carbon bond distances are almost equal, being 1.94(1) and 1.95(1) Å for molecule A and 1.97(1) and 1.95(1) Å for molecule B. They are slightly shorter than the corresponding distances found in the [Cu(hfac)(alkene)] family (between 2.013(5) and 2.277(7) Å in [Cu(hfac)(COD)][38,39] (COD = 1,5-cyclooctadiene) or 2.011(3) and 2.029(3) Å in [Cu(hfac)(7-*t*-BuO−NBD)][40] (7-*t*-BuO−NBD = 7-*tert*-butoxy-2,5-norbornadiene). It is not a surprising result, because one can expect a stronger interaction between the copper(I) and the carbon in the case of the alkyne family, because of its higher electron density (four π-electrons). The two C−C≡C angles are slightly different, 154.4(6)° and 146.5(5)° for A and 153.7(7) and 148.3(6)° for B, and not too far from the assumed linear geometry of the 'free' alkyne. The two independent C≡C distances in the complex are slightly different, being 1.16 (2) and 1.22 (2) Å, and are not appreciably elongated when compared to that of 'free' 2-butyne (1.211 Å).[41] The extent of σ and π back-bonding in η^2-alkyne metal complexes may be inferred from the C≡C bond lengthening and the extent of alkyl deformation (C≡C−R angles) from the linear geometry in the 'free' alkyne. On the basis of the relatively small disturbance of MHY in [Cu(hfac)(MHY)], we expect alkyne−copper bonding

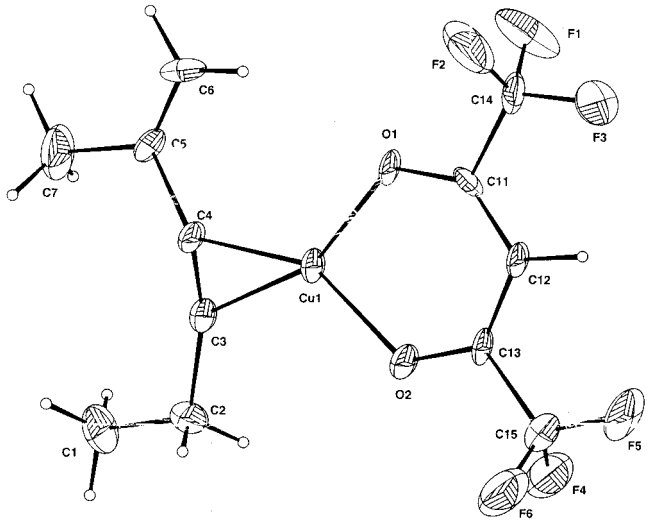

Figure 1. Representation of the X-ray crystal structure of [Cu(hfac)(MHY)], showing 30% probability thermal ellipsoids.

(36) Chen, T.-Y.; Cicoira, F.; Hoffmann, P.; Staufer, C.; Ohta, T.; Vaissermann, J.; Doppelt, P. Manuscript in preparation.
(37) Baum, T. H.; Larson, C. E.; May, G. *J. Organomet. Chem*. **1992**, *425*, 189.
(38) Chi, K. M.; Shin, H.-K.; Hampden-Smith, M. J.; Duesler, E. N. *Polyhedron* **1991**, *10*, 2293.
(39) Kumar, R.; Fronczek, F. R.; Maverick, A. W.; Lai, W. G.; Griffin, G. L. *Chem. Mater*. **1992**, *4*, 577.
(40) Chi, K.; M. Hou, H.-C.; Hung, P.-T. *Organometallics* **1995**, *14*, 2641.
(41) Pignataro E.; Post, B. *Acta Crystallogr*. **1955**, *8*, 672.

Table 3. Selected Experimental Interatomic Bond Lengths (Å) and Bond Angles (deg) for [Cu(acac)(MHY)], [Cu(hfac)(MHY)], [Cu(tfac)(MHY)], and [Cu(pfac)(MHY)] and the Corresponding Values of the B3LYP-Optimized Structures

	[Cu(acac)(MHY)]	[Cu(hfac)(MHY)]			[Cu(tfac)(MHY)]		[Cu(pfac)(MHY)]	
		exp						
	calc	A	B	calc	exp	calc	exp	calc
Cu−C3≡	1.967	1.94(1)	1.97(2)	1.988	1.941(5)	1.973	1.954(7)	1.988
Cu−C4≡	1.973	1.95(1)	1.95(1)	1.980	1.937(5)	1.967	1.957(7)	1.984
C≡C	1.270	1.16(2)	1.22(2)	1.265	1.224(8)	1.269	1.232(9)	1.264
C═C	1.355	1.28 (2)	1.35(3)	1.354	1.317(9)	1.354	1.33(1)	1.354
Cu−O1	1.945	1.950(9)	1.97(1)	1.966	1.939(4)	1.958	1.952(5)	1.969
Cu−O2	1.948	1.957(9)	1.98(2)	1.966	1.939(4)	1.955	1.957(4)	1.971
O1−Cu−O2	94.6	93.7(4)	94.2(4)	92.1	95.6(2)	93.3	93.4(2)	91.4
O1−Cu−C3	151.9	154.4(6)	153.7(7)	153.6	151.2(2)	152.1	154.3(2)	152.8
O2−Cu−C3	113.5	111.9(6)	122.0(6)	114.3	113.2(2)	113.5	112.3(2)	115.7
O1−Cu−C4	114.3	119.7(5)	117.4(6)	116.4	114.4(2)	114.3	117.6(3)	115.8
O2−Cu−C4	151.1	146.5(5)	148.3(6)	151.5	150.0(2)	151.9	149.0(2)	152.9
C3−Cu−C4	37.6	34.7(6)	36.4(7)	37.2	36.8(2)	37.6	36.7(3)	37.1
C2−C3−C4	159.0	163.2(15)	162.2(15)	160.8	161.0(6)	159.0	163.1(7)	160.9
C3−C4−C5	157.7	160.8(15)	157.8(15)	158.7	157.4(5)	157.7	158.7(7)	158.9
C4−C5−C6	121.3	125.1(16)	121.0(17)	121.7	121.5(5)	121.6	121.2(7)	121.9
Cu−O1−C11	125.0	122.5(9)	123.2(10)	125.7	121.1(3)	124.0	124.5(4)	127.1
Cu−O2−C13	125.1	124.5(10)	123.3(10)	125.7	124.0(3)	126.8	124.2(4)	127.0
Cu−C3−C4	71.0	73.2(10)	71.0(11)	71.7	71.4(3)	71.5	71.8(5)	71.6
Cu−C4−C3	71.5	72.2(9)	72.6(9)	71.1	71.8(3)	71.1	71.5(4)	71.3

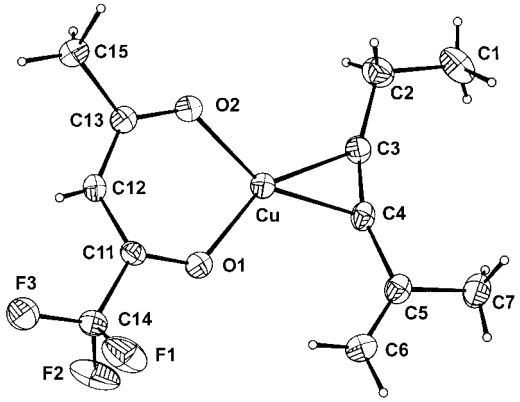

Figure 2. Representation of the X-ray crystal structure of [Cu(tfac)(MHY)], showing 30% probability thermal ellipsoids.

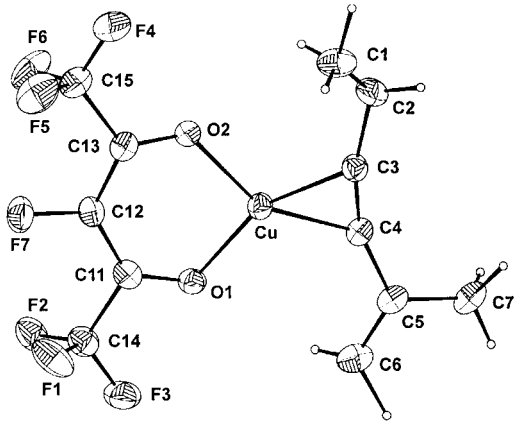

Figure 3. Representation of the X-ray crystal structure of [Cu(pfac)(MHY)], showing 30% probability thermal ellipsoids.

to be dominated by σ bonding (electron donation from the alkyne to the copper center) as in other [Cu(hfac)-(η^2-alkyne)] complexes. We will see that the theoretical study indeed supports this interpretation.

The structures of [Cu(tfac)(MHY)] and[Cu(pfac)-(MHY)] (Figure 2 and Figure 3 respectively) are almost identical to that of [Cu(hfac)(MHY)]. In all these structures, the coordination sphere around the Cu(I) ion is

Table 4. Deviations of Defining Atoms from the Best Molecule Plane in 0.01 Å for [Cu(hfac)(MHY)], [Cu(tfac)(MHY)] and [Cu(pfac)(MHY)]

	[Cu(hfac)(MHY)]		[Cu(tfac) (MHY)]	[Cu(pfac) (MHY)]
	molecule A	molecule B		
Cu	0.05	0.10	0.00	0.04
O1	0.04	0.02	0.00	0.08
O2	0.04	0.00	0.00	0.05
C1	−0.08	−0.02	0.00	−1.11
C2	0.11	−0.12	−0.01	−0.02
C3	0.05	−0.06	0.01	−0.03
C4	0.06	−0.07	0.01	−0.02
C5	0.01	−0.03	0.0	−0.04
C6	0.08	−0.31	0.01	−0.14
C7	−0.19	0.34	0.00	0.09
C11	0.04	0.17	−0.01	−0.01
C12	−0.07	0.13	0.00	−0.06
C13	−0.05	0.01	−0.01	−0.04
C14	−0.05	0.23	−0.01	−0.07
C15	−0.05	−0.39	0.01	−0.12

planar, and because of the conjugation between the C≡C and the C═C bonds, the entire molecules can be considered as roughly planar, as illustrated in Table 4, where we report the atom deviations in hundredths of an Å from the best calculated plane (except for the fluorine atoms). It is interesting to note that the [Cu-(tfac)(MHY)] structure is almost perfectly planar, with deviation values less than 0.02 Å, while for the other structures the deviation, certainly due to the packing, can be as high as 1.12 or 0.39 Å for sp^3 carbon atoms (C1 in [Cu(pfac)(MHY)], C15 in [Cu(hfac)(MHY)], respectively).

In these structures, the coordination sphere for the Cu and the C≡C bonds are poorly affected by the metal chelation and the free double bond is oriented toward the metal. Looking at the structures of [Cu(tfac)(MHY)], and[Cu(pfac)(MHY)] in more detail, they are much more precise than that of [Cu(hfac)(MHY)] and interesting features appear: the CH_2–C≡C and C≡C−C═ angles are slighty closer to the theoretical 180° value for [Cu-(pfac)(MHY)] than for [Cu(tfac)(MHY)] (respectively 163.0(7)°, 158.7(7)° and 161.0(6)°, 157.4(5)°), and the copper−alkyne−carbon bond distances are slightly

shorter in [Cu(tfac)(MHY)] than in [Cu(pfac)(MHY)], being respectively 1.941(5), 1.937(5), 1.954(7), and 1.957(7) Å, while the C≡C distances are almost identical (1.224(8) and 1.232(9) Å, respectively). Such a result has been previously found in the structures of [Cu(tfac)(P(CH$_3$)$_3$)][8b] and [Cu(hfac)(P(CH$_3$)$_3$)],[42] where the Cu−P distances were 2.133(2) and 2.142(3) Å, respectively. These values tend to sustain what we previously found: the Cu−alkyne bond is slightly stronger in [Cu(tfac)(MHY)] than in [Cu(pfac)(MHY)].

The ligand tfac being asymmetrical, some ancillary ligand bonds are not equivalent as previously reported.[8b] Due to the presence of the electroattractive CF_3 group, the C11−C12 bond (1.368(8) Å) is shorter than the C12−C13 bond (1.397(8) Å) and the C−CF_3 bond is longer and hence weaker than the C−CH_3 bond (respectively 1.523(7) and 1.498(8) Å).

In [Cu(pfac)(MHY)], two F atoms are present. Surprisingly, the F(7)−C_{sp^2} bond (1.351(8) Å) is slightly longer than the F−C_{sp^3} bond (CF_3, averaged at 1.30 Å), but such lengths are frequently found in CF_3-containing organic compounds.[43]

Theoretical Study of the Electronic Structure and Coordination Modes of the Family of [Cu(acac)alkyne] Complexes. We studied the four Cu(I) MHY complexes by modifying the other coordinated ligand: acac, tfac, hfac, and pfac. In each of the four cases, geometry optimization provides a minimum of energy with a planar coordination sphere for the Cu(I) atom (see Figures 1−3). The main structural parameters corresponding to the four optimized complexes are summarized in Table 3. The comparison with the available experimental data shows a good agreement, reflecting a good description of the intramolecular bonds. As said before, the alkyne coordination to the Cu(I) causes the loss of the triple C≡C bond character, as clearly indicated by the increase in the bond length (C3−C4 optimized bond distance is 1.211 Å for the free alkyne) and the C3−C4−C5 and C2−C3−C4 angle values with intermediate values between a double and triple bond. This result is also corroborated with the frequencies indicated in Table 2 showing that the calculated values (in good agreement with the experimental data) predict a reduction in the C≡C stretching of around 200 cm^{-1} for the coordination with the copper atom. These calculated values accurately reproduce the frequency shifts, corroborating the good description of this kind of interaction. We can propose a relationship using the isolobal analogies[44] between our alkyne complexes and a cyclopropene molecule, considering the fragment [Cu(acac)] as isolobal with a CH_2^{2+} unit.

A second coordination mode can be explored with the alkyne molecule perpendicular to the [Cu(acac)] plane (Figure 4). We searched for stationary points corresponding to this coordination, but we found neither transition states nor minima. To confirm these results, we repeated the calculations with other algorithms and codes,[29,30] but in all cases the only stationary point found is the planar structure. Due to this impossibility to obtain a true stationary point for the perpendicular coordination, we fixed this coordination environment for the Cu atom, and performing an optimization of the structure we were able to estimate the relative energy in comparison with the planar coordination. The results show that for these complexes, planar coordination is the most stable, with energy differences of 57.7, 44.9, 39.3, and 62.7 kJ/mol for the acac, tfac, hfac, and pfac complexes, respectively. The explanation of the relative stability of both coordination modes can be easily understood by a simple diagram of molecular orbitals (Figure 4). There is a larger stabilization of the planar coordination due to the stronger interaction of the alkyne π^* orbitals with the d_{xy} orbital in comparison with the d_{xz} orbital for the perpendicular coordination. Also, the bond with the acac ligand increases the hybridization of the p and the d_{xy} orbitals, enhancing the strength of the metal−alkyne bond. The same explaination may also be valid for the greater stability of the planar coordination of similar alkene complexes.[45]

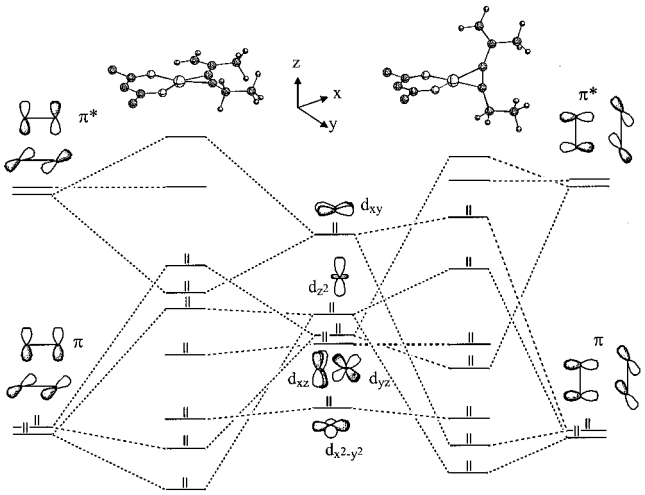

Figure 4. Molecular orbital diagram for two coordination modes of [Cu(β-diketonate)(MHY)]: (left) planar geometry and (right) tetrahedral one.

An interesting point is the effect of the substituents of the acac ligand on the relative stability of these complexes. Simple orbital analysis reveals that only the pfac appreciably modifies the composition of the orbitals due to the inclusion of the F atom in position 3 of the acac-type ligand. However, the orbital contribution of the fluorine atoms does not seem very relevant for the Cu−alkyne bond. Thus, to obtain a quantitative estimation of the stability of the Cu−alkyne bond, we calculated the interaction energies between the alkyne and the complex formed by the acac-type ligand and the Cu(I) cation. Unexpectedly, the results show an almost negligible influence of the acac substituents, the interaction energies being −175.6 kJ/mol for the acac and pfac complexes and −173.5 kJ/mol for the hfac and tfac ones.

We analyzed the preference of the multiple bonds in the MHY ligand in this type of complex to adopt a trans conformation. Our calculations show that for the acac ligand, the trans conformation is 8.3 kJ/mol more stable than the cis one. To understand why, we performed the

(42) Shin, H.-K.; Chi, K. M.; Farkas, J.; Hampden-Smith, M. J.; Kodas, T. T.; Duesler, E. N. *Inorg. Chem.* **1992**, *31*, 1, 424.
(43) Liebman, J. F.; Greenberg, A. *Molecular Structure and energetics*, VCH Publishers: New York, 1986; Vol. 3, Chapter 4, p 141.
(44) Hoffmann, R. *Angew. Chem., Int. Ed. Engl.* **1982**, *21*, 711.
(45) Isaacs, N. *Physical Organic Chemistry*; Logman Scientific & Technical: Essex, 1995; p 345.

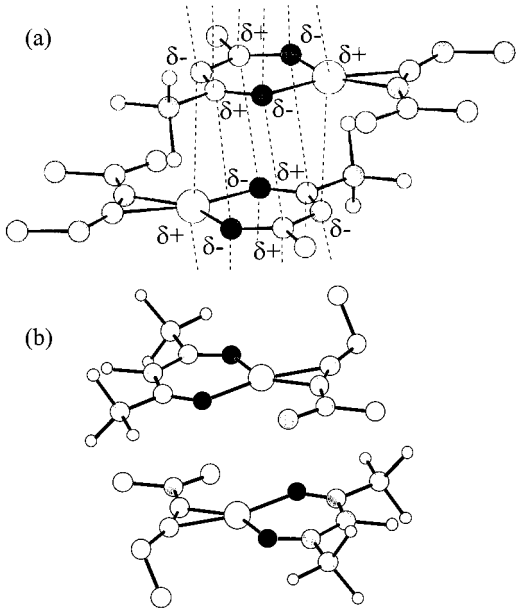

Figure 5. (a) Suggested intermolecular π-π interactions in the shifted stacked structure of [Cu(tfac)(MHY)]. (b) The almost perfect alternating structure of [Cu(pfac)(MHY)] due to a stronger dipolar moment coupling.

calculation for the isolated ligand with the two conformations, and the trans conformer is 5.4 kJ/mol more stable than the cis one. This agrees with the well-known preference of conjugated diene molecules for the trans conformation.[46] The increase of the relative stability in the formation of the copper complex can be understood due to the stronger C(sp^2)−H···O intramolecular hydrogen bond of the trans conformer (found in the [Cu(pfac)(MHY)] structure) in comparison with the C(sp^3)−H···O bond in the cis one (found in the [Cu(tfac)(MHY)] and [Cu(hfac)(MHY)] structures).[46]

As said before, the decomposition of such compounds gives Cu(0), MHY, and a [Cu(β-diketonate)$_2$] complex and indicates a similar thermodynamic stability of the products. However, experimentally, the complex with the pfac ligand shows a higher stability, while the acac complex decomposes easily. To explain this trend, we analyzed the intermolecular effects and found two relevant factors. The first is related to the presence of fluorine atoms in the acac ligand, which provide a higher stability due to the formation of hydrogen bonds with the neighboring molecules, and the second is related to the different dipolar moments of each molecule. The pfac compound adopts a nonregular stacked structure with short and long Cu···Cu distances of 3.915 and 4.246 Å, with one molecule oriented in the opposite direction to its neighbor, giving alternating stacking, examples of which are given in Figure 5. There are several weak hydrogen bonds,[47] the shortest H···F distances being 2.420 Å between the stacks and 2.591 Å with the neighboring stacked molecule. The shortest H···F distance (2.420 Å) corresponds to the interaction of the F in the β-diketonate 3 position. Consequently, this interaction will not be present in the acac, tfac, and hfac compounds. Thus, the structure of the hfac compound trends to maximize the interaction of the copper atom with the triple bond of the neighboring molecule adopting an eclipsed stacking. The shortest H···F distances found in the structure are relatively longer than for the pfac one, 2.887 Å for the interstack interaction while it is 2.798 Å for the intrastack one. This analysis agrees well with the higher stability of the pfac compound found experimentally.

Table 5. Calculated Vertical Excitation Energies (nm) and Oscillator Strengths (in parentheses) for the Four Complexes Using the TDDFT Method with the B3LYP Functional Complexes Considering Only the Most Intense Spin-allowed Transitions[a]

	[Cu(acac)(MHY)]	[Cu(tfac)(MHY)]	[Cu(hfac)(MHY)]	[Cu(pfac)(MHY)]
MLCT	**305 (0.0246)**	**281 (0.0434)**	**318 (0.0229)**	329 (0.0313)
MLCT	272 (0.0331)	270 (0.1269)	**299 (0.0891)**	304 (0.0957)
MLCT	**257 (0.0930)**	**249 (0.0219)**	260 (0.1209)	276 (0.1154)
MLCT	**242 (0.2032)**	**243 (0.1316)**	**240 (0.1588)**	240 (0.1096)
exp		306	317	346

[a] In bold, we have indicated the MLCT that are mainly transferred to the β-diketonate ligand, otherwise the transfer is from the metal to the alkyne.

For the acac compound, the X-ray diffraction structure is not available, but we performed a geometrical optimization of a dimer to elucidate some structural information. The optimized geometry corresponding to the alternated stacking is 10.5 kJ/mol more stable than the eclipsed one. The stacking adopts an orientation that favors the interaction between the copper atom and the triple bond of the neighboring molecule as for the hfac compound, but in this case, due to the alternating stacking, there are two Cu···alkyne interactions instead of one in the hfac structure. The presence of such interactions could facilitate electron transfer between the copper atoms, leading to the easier decomposition of the acac compound in comparison with the other three. Such interactions (as seen in Figure 5) become weaker with increasing n_F, because electroattracting fluorine atoms decrease the Cu(β-diketonate) electron density, lending to produce both more volatile and more stable compounds.

The calculated dipolar moments are 0.6, 4.8, 5.0, and 7.2 D for the acac, tfac, hfac, and pfac structures, respectively. The obtained trend of the dipolar moment correlates well with the stability order found experimentally for the four complexes. The dipolar moment coupling affects the π-π interactions, as seen in Figure 5: for [Cu(tfac)(MHY)], the molecules are in a shifted alternating stack, while for [Cu(pfac)(MHY)], the molecules alternate almost perfectly. In conclusion, the existence of both H···F hydrogen bonds and dipole moments has a significant effect on the stability of the complexes but not on their volatility.

We performed a theoretical study of the spectra of the electronic transitions of theses complexes using time dependent density functional theory. The results for the spin-allowed transitions are summarized in Table 5. These correspond to metal ligand charge-transfer excitations (MLCT) as expected for the d^{10} configuration of the Cu(I) ion. For most of these electronic transitions, the excited state corresponds to a charge transfer to the β-diketonate ligand, because the LUMO is mainly centered in this ligand. We note that the presence of

(46) Desiraju, G. R.; Steiner, T. *The Weak Hydrogen Bond in Structural Chemistry and Biology*; Oxford University Press: Oxford, 1999; Vol. 9.

(47) Howard, J. A. K.; Hoy, V. J.; O'Hagan, D.; Smith, G. T. *Tetrahedron* **1996**, *52*, 12613.

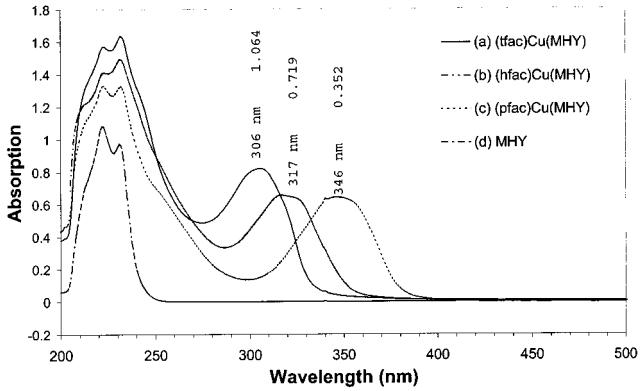

Figure 6. UV−vis spectra of a 10^{-4} M pentane solution of (a) [Cu(tfac)(MHY)], (b) [Cu(hfac)(MHY)], (c) [Cu(pfac)(MHY)], and (d) free MHY.

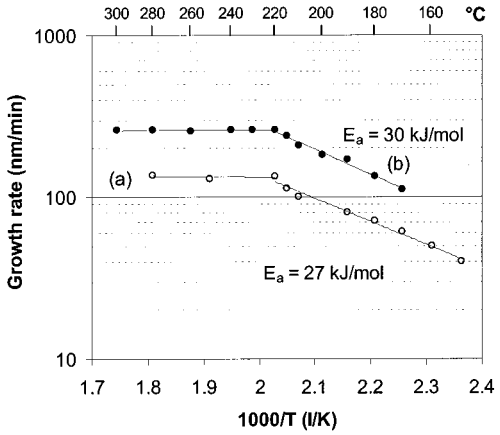

Figure 7. Copper CVD growth rate using [Cu(hfac)(MHY)] on TiN substrates as a function of the substrate temperature for two precursor flows, 0.23 (a) and 0.46 g/min (b).

fluorine atoms in the β-diketonate ligand shifts to longer wavelengths, probably due to their greater electronegativity, which lowers the energy of the empty orbitals corresponding to those ligands. The experimental spectrum of [Cu(hfac)(MHY)] (see Figure 6) is in excellent agreement with the calculated values, showing that the TDDFT[48] approach is very useful for the analysis and assignment of UV−visible spectra. Thus, we can note that the inclusion of fluorine atoms in the acac ligand produces an increase in the wavelengths, probably due to their greater electronegativity in comparison with the hydrogen atoms, and consequently lowers the empty orbitals corresponding to these ligands.

CVD of Copper Thin Films by Direct Liquid Injection Using [Cu(hfac)(MHY)]. We focused our deposition work on [Cu(hfac)(MHY)], which is by far the best precursor of the series. The dependence of the growth rate on substrate temperature for two different precursor flows of 0.23 and 0.46 g/min is shown in Figure 7 displayed as an Arrhenius plot. Two regions can be easily observed: a saturation region, i.e., the mass-flow-controlled regime above 200 °C, and a region below this temperature where the temperature dependence is relatively strong, i.e., the surface-reaction-limited regime. The transition between the two regions is not dependent on the precursor flow as it is for the growth rate, which is simply doubled for a given temperature when the precursor flow is doubled. The activation energy of the surface reaction can be deduced from the slope of the curve in the reaction-controlled regime. The values obtained are 27 and 30 kJ/mol for a precursor flow of 0.23 and 0.46 g/min, respectively, which are very close when considering the measurement precision (estimated at ±10%). These activation energies are rather low when compared to those of other precursors: the activation energy for [Cu(hfac)(COD)] (COD = 1,5-cyclooctadiene) was measured by Reynolds et al.[8a] as 124.6 kJ/mol (at 18 mTorr) and by Park et al.[7d] as 61.9 kJ/mol for [Cu(hfac)(VTMS)] and 62.7kJ/mol for [Cu(hfac)(ATMS)] (ATMS = allyltrimethylsilane) at 0.5 Torr and more recently by Kröger et al.[49] as 80.7 kJ/mol for [Cu(hfac)(VTMS)] at 1.5 Torr. To our knowledge, the lowest activation energy reported so far was 31 kJ/mol for [Cu(hfac)(VTMOS)][7b] (where VTMOS = vinyltrimethoxysilane) at 6 Torr. In this last case, it has been suggested[50] that oxygen atoms of the alkoxysilyl groups help the absorption of the precursor by interacting with the substrate and hence lower the activation energy of the whole process. In the case of [Cu(hfac)(MHY)], such interaction is possible through the free double bond, which can interact strongly with the copper atoms at the surface, facilitating both the absorption of the precursor and the disproportionation reaction and lowering the process activation energy. Further studies are needed to confirm this interpretation.

Growth temperature has a strong impact on the microstructure of copper films obtained from the pyrolysis of [Cu(hfac)(MHY)]. SEM micrographs of as-deposited morphologies of copper films grown at eight temperatures from 170 to 300 °C are shown in Figure 8. In general, increasing growth temperature resulted in an increase in the average grain size, with an increasing degree of voids in the film. It can be seen that grain size is uniform at 200 °C and that intergrain connectivity is high. As growth temperature is increased, some grains grow at the expense of others, leading to a broader distribution of grain sizes: considerably larger grains (>1 μm) are mixed with much smaller ones (∼0.2 μm), as shown in Figure 8g. As shown in Figure 8h, well-developed facets characteristic of the fcc structure appear at a growth temperature of 300 °C. Faceting, together with the concomitant void structure, sharply reduces intergrain connectivity, leading to higher electrical resistivity. As the electrical resistivity of films depends on their microstructure, room-temperature electrical resistivity was measured for copper films grown at different temperatures (Figure 9). The resistivity values are almost independent of the film thickness, being in the range 500−1000 nm. A minimum resistivity of 2.3 μΩ cm was achieved at a growth temperature of 200−210 °C, which corresponds to the transition temperature between the mass-flow-controlled and the surface-reaction-limited regimes. Resistivity of films increases steadily as the growth temperature is raised above 230 °C and reaches a value of 8 μΩ cm at 300 °C. The high resistivity of the copper

(48) Vidal, S., PhD, Ecole Nationale Supérieure de Chimie de Toulouse (France), 1999.

(49) Kröger, R.; Eizenberg, M.; Cong, D.; Yoshida, N.; Chen, L. Y.; Ramaswarmi, S.; Carl, D. *J. Electrochem. Soc.* **1999,** *146,* 3248.

(50) Nakamura, K.; Fugu, M.; Tachibana, A. *AMC 98, MRS Proceedings* **1999**, 153.

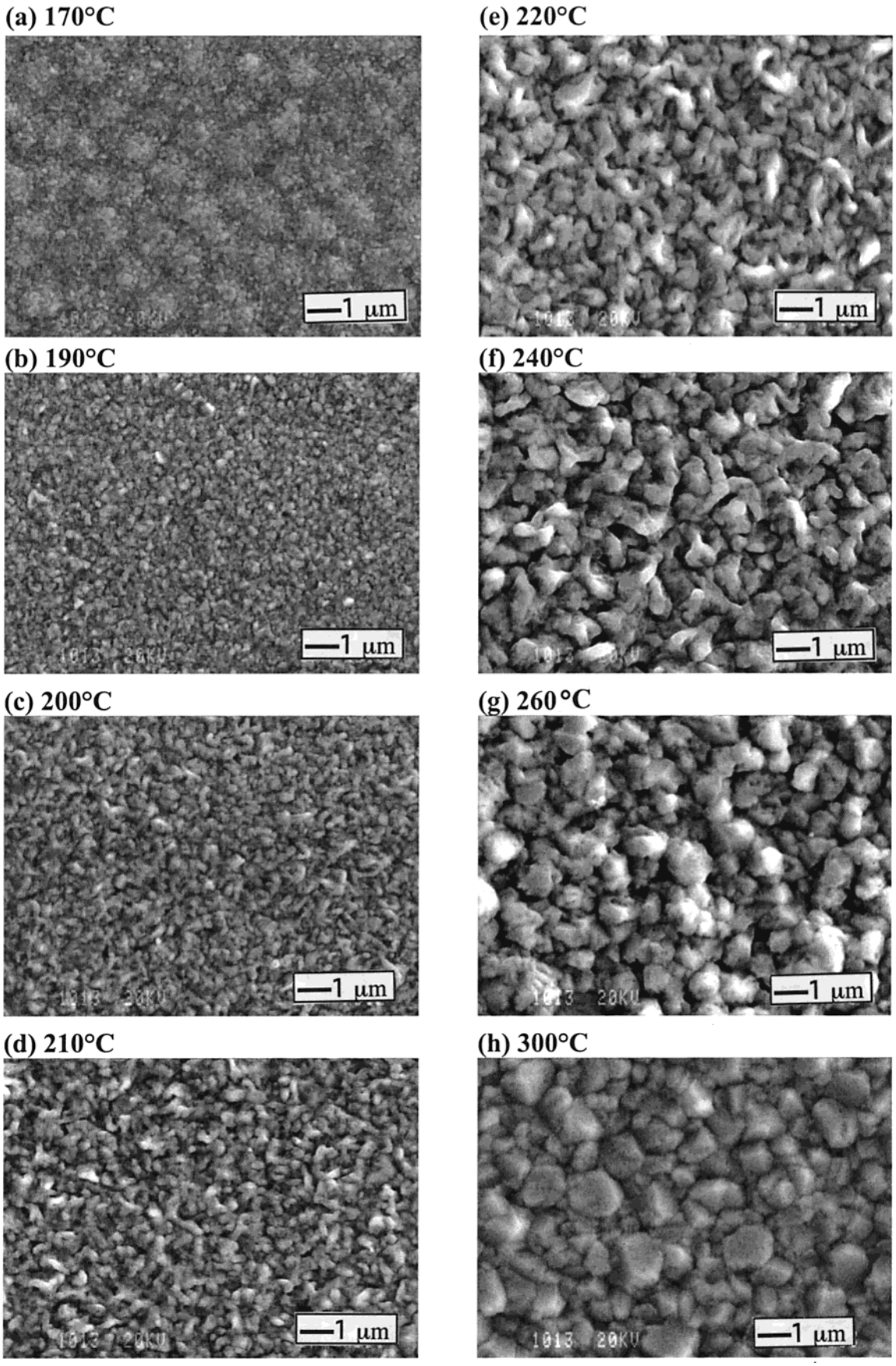

Figure 8. SEM pictures of the copper films obtained by CVD using [Cu(hfac)(MHY)] at different temperatures on TiN under 2 Torr for a precursor flow of 0.46 g/min.

film grown at high temperature reflects the poorly connected grain structure of the film or its higher impurity content. At growth temperature below 200 °C, the resistivity increases, probably because of higher

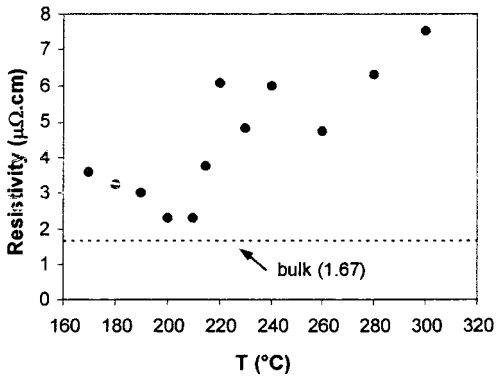

Figure 9. Variation of the resistivity of CVD copper films using [Cu(hfac)(MHY)] with deposition temperature. The precursor flow was 0.46 g/min.

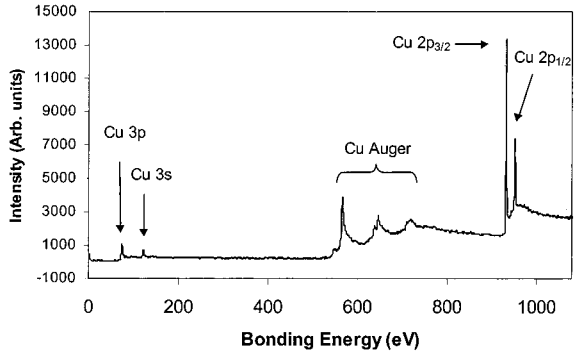

Figure 10. XPS spectrum after 10 min of Ar sputtering of a copper CVD film (obtained with [Cu(hfac)(MHY)]) on TiN at 220 °C for a precursor flow of 0.46 g/min.

concentration of grain boundaries leading to smaller size copper grains.

ESCA of a copper film obtained with a substrate temperature of 220 °C revealed that the film contained O and C (30.0 and 15.1 atom %, respectively) near the surface. A single argon ion sputter (4 kV for 10 min) is sufficient to completely remove the C and most O species, leaving an essentially pure Cu film, as shown in Figure 10, contaminated with a small amount of O species (2.7 atom %). Thus, the O and C probably represent surface impurities that result from air exposure between the CVD process and insertion into the ESCA system. The residual O impurities may come from a small leak or residual H_2O in our CVD setup and may explain the slightly higher values obtained for the resistivities of the copper films (~4 $\mu\Omega$ cm for a deposition temperature of 220 °C; see Figure 9). Nevertheless, the ESCA spectrum given in Figure 10 is very close to that of pure copper. Moreover, lower O content and resistivities have been reported on other equipment using a bubbler[14,48] or an injector[16] with the same precursor.

XRD was used to evaluate the preferred orientation of the Cu on CVD TiN, using the intensity ratio I_{111}/I_{200} of the Cu(111) and Cu(200) peaks. The ratio should be 2.17 for randomly oriented Cu.[51] The intensity varies slightly with the deposition temperature: from 2.8 at 170 °C, the ratio decreased to 2.2 at 220 °C, with a plateau up to 230 °C, where the ratio increased slowly up to 3.8 for 300 °C. Hence, around 220 °C the copper film grows randomly on TiN. Such results are very similar to what has been obtained for TiN using [Cu(hfac)(ATMS)].

Scratch tests have been used to roughly evaluate the adhesion of the copper film on the TiN layer. Some prelimary results have been given by another group using the same precursor and a comparison of various precursors was made. We checked the adhesion of the film with deposition temperature. For the films deposited above 260 °C, the adhesion was poor, probably due to the presence of rather large grains, whereas for temperatures <220 °C, the copper film stayed on the substrate, demonstrating that the adhesion of the film on TiN exceeded the adhesion of the tape to the film. For deposition temperatures between 220 and 260 °C, the film was partially removed from the substrate. As the adhesion of the copper film is critical for the use of the precursor in the microelectronics industry, further studies on structured wafers are necessary to complete these prelimary studies. Such studies are now underway.

Conclusion

Four new β-diketonate Cu(I) complexes with a MHY Lewis base have been reported in this study. They are all heat-unstable, yielding Cu(0), free MHY, and [Cu(β-diketonate)$_2$] complexes. However, experimentally, the complex with the pfac ligand showed greater stability, while the acac complex decomposed most easily. We found that the stability of such complexes does not depend on the bonding strengh of the (η^2-C≡C)−Cu, which is only slightly affected by the number of fluorine atoms present on the β-diketonate ligand, but rather on weak intermolecular interactions such as the fluorine−hydrogen bonds detected in the X-ray structures. In the case of the complex containing perfluoroacetylacetonate, much stronger bonds were detected between the 3-F in the ancillary ligand and a hydrogen of the MHY ligand of another molecule. This explains why the corresponding complex is less volatile than [Cu(hfac)(MHY)], even though it contains more fluorine atoms.

Hence, the most interesting complex of the series is [Cu(hfac)(MHY)], which was studied for the chemical vapor deposition of copper films. Because of its stability, this new precursor is easily synthesized and handled, which is interesting for large-scale synthesis of the material and for its use in a fab environment. Moreover, quasi-pure copper films were obtained at a high growth rate of 260 nm/min. The activation energy for the surface-reaction-limited regime is only 30 kJ/mol, which suggests that the free double bond can play a role in the way that the molecule is absorbed on the surface. Our expectation is that the mode of absorption of our precursor could prevent the formation of the carbon and fluorine containing interlayer that is deposited at the TiN/Cu interface when Cu(hfac)(VTMS)] is used, reducing the adhesion of the copper film.[52] Such studies are now being undertaken on patterned wafers.

Acknowledgment. We are grateful to R. Madar (INPG, Grenoble, France) for his contribution at an

(51) JCPDS Standart Diffraction File no. 4-0838.

(52) Weiss, K.; Riedel, S.; Schulz, S. E.; Gessner, T. *AMC 98, MRS Proceedings* **1999**, 171.

early stage of the work. T. Ohta, P. Hoffmann, and F. Cicoira (EPFL, Switzerland) are thanked for the vapor pressure measurements and C. Jallabert and C. Chassagnard (ESPCI) for the NMR data. We are grateful to JIPELEC for having lent the JIPELEC INJECT liquid delivery and vaporization system and for technical support and assistance.

Supporting Information Available: Atomic coordinates and isotropic thermal parameters, bond distances, bond angles, anisotropic thermal parameters, H atom coordinates, and isotropic thermal parameters. This material is available free of charge via the Internet at http://www.pubs.acs.org.

CM0012318